

A new force sensor incorporating forcefeedback control for interfacial force microscopy

Stephen A. Joyce and J. E. Houston

Citation: [Review of Scientific Instruments](#) **62**, 710 (1991); doi: 10.1063/1.1142072

View online: <http://dx.doi.org/10.1063/1.1142072>

View Table of Contents: <http://scitation.aip.org/content/aip/journal/rsi/62/3?ver=pdfcov>

Published by the [AIP Publishing](#)

Articles you may be interested in

[Electrostatic force-feedback force sensor incorporated in an ultrahigh vacuum force microscope](#)
Rev. Sci. Instrum. **71**, 133 (2000); 10.1063/1.1150147

[Scanning force microscopy in the dynamic mode using microfabricated capacitive sensors](#)
J. Vac. Sci. Technol. B **14**, 901 (1996); 10.1116/1.589171

[Pt:SnO₂ thin films for gas sensor characterized by atomic force microscopy and xray photoemission spectromicroscopy](#)
J. Vac. Sci. Technol. B **14**, 1527 (1996); 10.1116/1.589132

[Atomic force microscopy stress sensors for studies in liquids](#)
J. Vac. Sci. Technol. B **14**, 1383 (1996); 10.1116/1.589103

[Forcebalancing force sensor with an optical lever](#)
Rev. Sci. Instrum. **66**, 5532 (1995); 10.1063/1.1146080

Nor-Cal Products



Manufacturers of High Vacuum
Components Since 1962

- Chambers
- Motion Transfer
- Flanges & Fittings
- Viewports
- Foreline Traps
- Feedthroughs
- Valves



www.n-c.com
800-824-4166

A new force sensor incorporating force-feedback control for interfacial force microscopy

Stephen A. Joyce and J. E. Houston
Sandia National Laboratories, Albuquerque, New Mexico 87185

(Received 30 August 1990; accepted for publication 19 November 1990)

A new interfacial-force microscope capable of measuring the forces between two surfaces over the entire range of surface separations, up to contact, is described. The design is centered around a differential-capacitance displacement sensor where the common capacitor plate is supported by torsion bars. A force-feedback control system is incorporated which balances the interfacial forces at the sensor, maintaining the common capacitor plate at its rest position. This control therefore eliminates the instability or "jumping" which occurs with conventional cantilever-based force sensors when the attractive force gradient between the fixed sample and sensor exceeds the mechanical stiffness of the cantilever. The operating characteristics of the sensor and its ability to measure interfacial forces using the feedback control at surface separations smaller than this instability point are demonstrated.

I. INTRODUCTION

Since its introduction, the atomic-force microscope (AFM)¹ has become a widely used tool for imaging surfaces on a microscopic scale. The popularity of the technique is due in large part to the fact that the AFM measures the force (or force gradient) between a sharp metal "tip" and a sample surface as opposed to the tunneling current measured with the scanning tunneling microscope (STM). Therefore, the AFM can image insulating as well as conducting samples. In addition to its imaging capability, the AFM also offers the possibility of measuring the strength of the interfacial interaction as a function of separation. A knowledge of the behavior of the interfacial force over the entire range of separations is of fundamental importance to obtaining a detailed understanding of such phenomena as adhesion, fracture, and tribology. Although the AFM is capable of measuring forces between microscopic surfaces at the pN (picoNewton) level, its primary application has been toward surface imaging, and there have been only a few experimental studies which specifically address the behavior of interfacial forces with separation.²⁻¹⁰

A large number of studies have investigated interfacial forces, particularly in the presence of liquids, using the crossed cylinder, surface-force apparatus (SFA) pioneered by Tabor and Winterton¹¹ and refined by Israelachvili.¹² The SFA measures forces over macroscopic areas, thereby requiring smooth, flat surfaces of large area—a nontrivial requirement.

As presently configured, both the SFA and the AFM consist of a fixed sample and a probe mounted on a cantilever beam of known stiffness. Normally, the probe is a mica sheet in the SFA and an electrochemically etched metal tip in the AFM. Interfacial forces are determined by measuring the deflection of the cantilever when the probe is in the proximity of the fixed sample. An instability in the cantilever-probe-sample potential occurs when the probe-sample force gradient, $\partial F/\partial z$, where z is the surface separation, exceeds the force constant of the cantilever. This

instability leads to the discontinuous movement of the probe into virtual contact with the sample. This behavior, commonly referred to as "jumping" or "snapping," has been described in detail by a number of groups.^{6,13} For many systems of interest, jumping may occur at surface separations ranging from a few Å up to hundreds of Å depending on the stiffness of the spring and the nature of the interfacial forces. Since the instability point in a given system is determined by the cantilever force constant, the surface separation at which jumping occurs can be made smaller by making the cantilever force constant larger.^{4,12} This, however, limits the force sensitivity of the apparatus which is necessary for measuring the weak forces present at large surface separations. The instability, therefore, precludes measurement of the interfacial forces over the broad range of separations required to perform a detailed characterization of surface-surface interactions.

In this article, we describe a new sensor for measuring interfacial forces which incorporates a force-feedback control to avoid the instability associated with conventional techniques. This scheme permits the determination of interfacial forces over the entire range of surface separations, from very large up to actual repulsive contact. In Sec. II, the concept of the new sensor is discussed, while Secs. III and IV describe the design and performance of the new interfacial force microscope incorporating the force-feedback sensor.

II. FORCE BALANCE APPROACH

The mechanical instability encountered in deflection force sensors occurs when $\partial F/\partial z$, the force gradient between probe and sample, exceeds k , the sensor force constant. The instability can be avoided, however, by balancing the interfacial force on the probe with an equal and opposite force. The net result is to keep the probe's position rigidly fixed in space as the sample is moved into proximity. Of course, this scheme only applies to the macroscopic aspects of the force sensor. On an atomic level, at separations on the order of 1 Å, a similar instability occurs when

the force gradient exceeds the effective elastic constants of the tip and sample materials.¹⁴⁻¹⁷ Feedback techniques cannot prevent this atomic-level instability.

Two previous publications have reported the use of force-balance schemes employed to measure interfacial forces.^{9,18} The first is a modified SFA where the probe is mounted on one end of a torsion balance; the initial displacement of the probe is monitored using optical interference techniques and then counterbalanced by inductive forces.¹⁸ The second method employs a modified AFM which uses the tunneling current from a tip located behind the cantilever to measure displacements.⁹ The important feature of this latter microscope is the ability to reposition the cantilever support so that the probe remains fixed at the same position in space, effectively varying the spring constant. We have developed a new force balance scheme based on a differential capacitance sensor which has the unique feature that the capacitor acts both as the displacement detector, through changes in capacitance, and as the counterbalance by the application of electrostatic restoring forces.

The use of capacitors as displacement transducers is, of course, not new.¹⁹ They have been used for years in accelerometers and have recently been employed in atomic force microscopes.^{20,21} Indeed, it has been suggested that capacitors are, in principle, the most sensitive electromechanical transducers.²² In a typical capacitance transducer, one plate is fixed while the other is free to move in response to an external force. The movement of the free plate changes the capacitor spacing or gap and therefore results in a change in the capacitance. A feature that, to our knowledge, has not been previously exploited is the ability to balance the forces on the free plate by applying a voltage, V , to the fixed plate. This voltage results in an electrostatic force, F_c , on the free plate, which is given by $F_c = CV^2/2d$ and is always attractive. Thus only external forces which are in opposition to the capacitance force can be counterbalanced. However, not all interfacial forces are expected to be attractive, even in the noncontacting region where, for example, repulsive "hydration" interactions between hydrophobic surfaces have been observed.²³

We circumvent this problem by using a differential capacitor as the sensor element. Thus, net repulsive forces on one capacitor, which cause the gap to decrease, can be counterbalanced by applying the restoring force to the other capacitor where the gap has increased. The differential capacitance sensor in our design is comprised of two fixed plates above which is suspended a common plate (a "teeter-totter"), free to rotate about supporting torsion bars. A schematic is shown in Fig. 1.

There are additional advantages to a differential capacitance scheme. For example, it lends itself naturally to use in an ac bridge. Bridge methods have the advantage of being null detectors where the output signal is proportional to the difference in the capacitance of the two legs, not the total capacitance; therefore, very small changes (on the order of 1 ppm) in capacitance are readily detected.

As a sample is brought into proximity of a tip mounted on one end of the teeter-totter, the interfacial forces cause

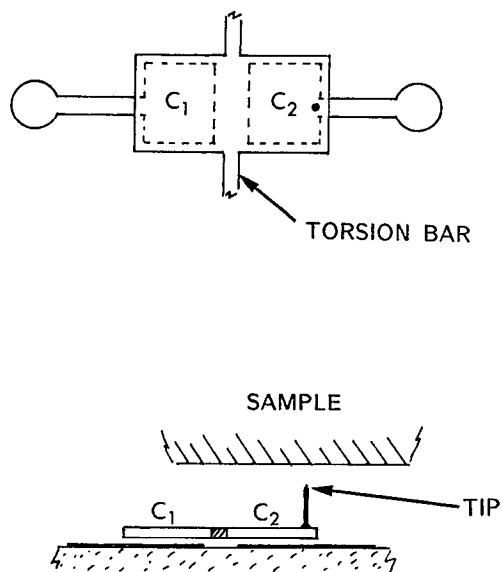


FIG. 1. The differential-capacitance force sensor consists of a common capacitor plate suspended by torsion bars above two separate counter plates. Interfacial forces between the tip and sample rotate the common plate and change the two capacitance values differentially.

a deflection, Δd at that end of the common plate. $\Delta d = F_i/k$, where F_i is the interfacial force and k is the linear force constant of the torsion bars. The change in the gap, Δd , on one end results in an opposite displacement, $-\Delta d$, on the other. These changes will unbalance the bridge resulting in an output voltage proportional to $\Delta C/C = \Delta d/2d$ (so long as $\Delta d \ll d$). The factor of 2 arises from the fact that the capacitor gap is fixed at the torsion bars and d is measured from the end of the teeter-totter. Therefore, the average gap varies by only $\frac{1}{2}$ the value of d .

The bridge imbalance can be fed to an electronic feedback loop that rebalances the bridge by applying a dc voltage to one of the fixed plates. The force-feedback scheme prevents "jumping" by maintaining the common plate at its rest position and allows an electronic determination of the interfacial force through the magnitude of the applied dc voltage.

Another advantage of a differential-capacitance sensor is its relative immunity to certain environmental factors. In particular when operated in air, small changes in the humidity or temperature can have a significant effect on the capacitance by changing the dielectric constant of the capacitor gaps. These effects are expected to be uniform and effectively cancel in the differential design. In addition, this design has a greater immunity to vibrations since only vibrations which differentially change the gap will be detected. And finally, the differential scheme effectively balances noise present on the function generator driving the bridge.

III. DESIGN

The current prototype sensor, shown schematically in Fig. 2, was fabricated using standard thin film techniques. The base, consisting of the two fixed plates, a ground plane

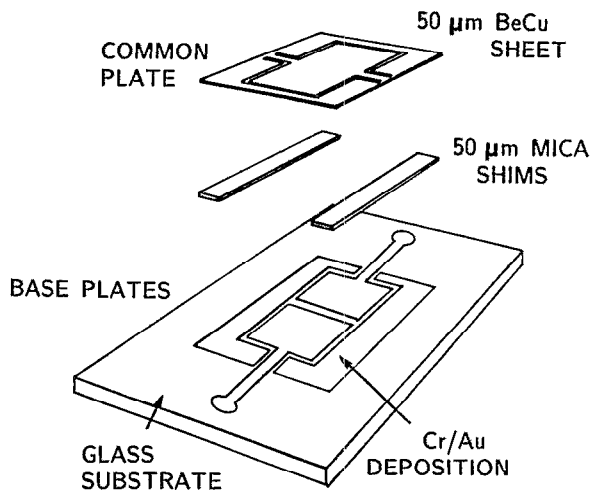


FIG. 2. A schematic illustration of the prototype force sensor. The common capacitor plate and torsion bars are photomasked and etched from a 50 μm BeCu sheet while the two counter plates are deposited, photomasked and etched on a glass substrate (200 \AA Cr followed by 1000 \AA Au). The capacitor spacing is established by two 50 μm mica shims.

and connector pads, is made by depositing a 200 \AA Cr + 1000 \AA Au film on a photomasked glass plate. A subsequent wet etch produced the pattern illustrated in Fig. 2. The common capacitor plate (teeter-totter plus torsion bars) was photomasked and etched from a 50 μm thick Be-Cu sheet. The gap was determined by 50 μm mica shims glued between the base and common plate. The individual capacitor plates have areas of 10 mm^2 yielding capacitance values of ~ 1.5 pF. The torsion bar dimensions were 6.3 $\text{mm} \times 150 \mu\text{m} \times 50 \mu\text{m}$, giving a calculated force constant, k , of ~ 13 N/m.

Since the bridge imbalance produces output voltages proportional to $\Delta d/2d$, greater displacement sensitivity can be achieved by reducing the capacitor gap. In the present design, the minimum gap is limited by the mechanical stability of Be-Cu common plate. Ultimately, the displacement sensitivity is determined by the thermally excited vibrational amplitude of the teeter-totter, $A_T = (2k_B T/k)^{1/2}$ (Ref. 4). The calculated A_T for the prototype in Fig. 2 is calculated to be 0.02 nm.

The electronics associated with the ac bridge and the feedback are shown schematically in Fig. 3. The ac voltage from a frequency generator first passes through a balanced rf transformer. The bridge drive voltage was 7 V rms and the bridge frequency, although variable, was normally $f_B = 2.5$ MHz. A variable capacitor is used to balance the small natural imbalance of the differential capacitor and stray capacitance. Tuning the bridge to better than 1 part in 10^5 (i.e. to $\Delta C < 10^{-17}$ F) can be tedious with the mechanical variable capacitor. However, the use of voltage-variable-capacitance diodes²⁰ (varactors) was found to produce significant amounts of electrical $1/f$ noise.

The imbalance signal from the common capacitor plate is fed to a close-coupled preamp and finally to an EG&G Model 5202 high-frequency lock-in amplifier. The use of the preamplifier is necessary since the signal from the 1.5

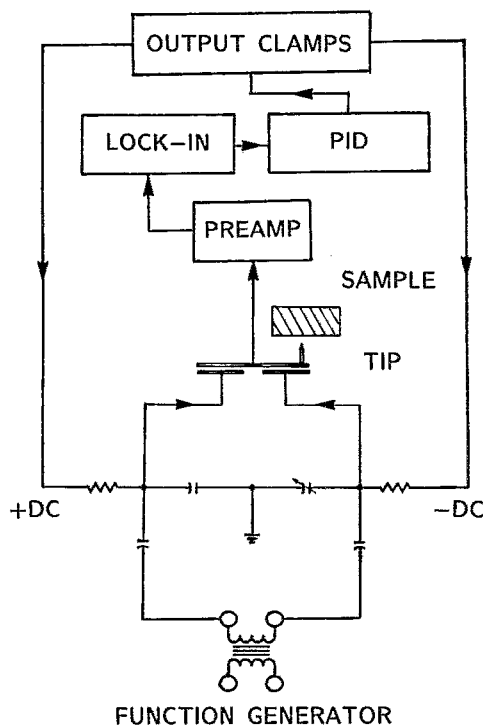


FIG. 3. A schematic of the force-feedback control system. The ac bridge imbalance is measured by a low-input capacitance preamp and lock-in amplifier. The force-feedback is implemented by a proportional-integral-derivative controller and two active diode clamps to guide the dc feedback voltage to the proper capacitor plate.

pF bridge would be significantly reduced by the cable and lock-in input capacitances. The preamplifier used has been described in detail by Neubauer *et al.*²⁰ The use of phase-sensitive detection permits the monitoring of only the in-phase, reactive, component of the signal in the presence of the out-of-phase, resistive component. The out-of-phase loss signal eventually overloads the lock-in and sets an upper limit on the bridge drive frequency, since the loss of capacitors generally increases as the frequency is increased.

The output of the lock-in, normally operated at a gain of 10^3 , represents the input to the feedback controller. The control circuit consists of a simple proportional-integral-derivative (PID) controller, which is unique only in its output circuitry. As mentioned above, the electrostatic restoring force does not depend on the sign of the applied voltages. The sign of the imbalance voltage is important, however, in determining to which fixed plate the dc voltage is to be applied. The output stage of the controller directs the application of the dc voltage through the use of two active diode clamps.²⁴ The clamp attached to C_1 passes voltages resulting from positive sensor displacements while the other clamp passes voltages to C_2 resulting from negative bridge displacements.

IV. PERFORMANCE

Several tests were performed to determine the overall capabilities of the force feedback, differential-capacitance sensor. In the first, mechanical-displacement tests were

performed by attaching a W tip to a piezo tube and electrically ramping the tip after it had made mechanical contact with one end of the sensor. The bridge response to the mechanical deflections were found to be linear, within the noise, over the measurement range of deflection of approximately $1 \mu\text{m}$. The minimum detectable deflection for a measurement time constant of 1 ms was found to be $\sim 5 \text{ \AA}$.

Ideally, the signal-to-noise ratio for a bridge circuit of the type used here is given by the expression,²⁵

$$S/N = [v_0 / (e_s + e_n)] [C / (C + C_i)] [1 / \Delta f]^{1/2},$$

where v_0 is the bridge drive voltage, C is the individual teeter-totter capacitance, C_i is the total input capacitance of the preamplifier (including cabling, etc.), e_s is the voltage shot noise corresponding to the signal current entering the base circuit of the initial-stage transistor, e_n is the electronic noise present in the system, and Δf is the overall system bandwidth. Under ideal conditions, e_n is dominated by white noise generated by the preamplifier and consists of shot noise from the base-bias current and the voltage noise produced in the first-stage transistor.²⁰

For our preamp, the value e_n for the MPHS10 first-stage transistor is given as $\sim 10 \text{ nV}$. Thus with an overall system bandwidth of 1000 Hz, the displacement sensitivity predicted from noise considerations is 0.04 \AA . This value is to be compared with the $\sim 5 \text{ \AA}$ figure obtained from noise measurements and the 0.2 \AA value predicted earlier from the thermal vibrations of the sensor. The reason for the discrepancy between these figures is partly due to mechanical vibrations of the system and partly to extraneous electronic noise. A spectral analysis of the overall electronics noise shows a dominance by 60 Hz (and its overtones) and by 305 Hz, which was found to be generated by the lock-in amplifier. Careful attention to circuit design and the elimination of the lock-in contribution should result in a significant improvement of the system performance to that near the ideal indicated above.

Electrostatic displacement tests were performed by applying a dc voltage to one of the fixed plates and measuring the resulting bridge imbalance. These results are presented in Fig. 4 showing the expected $(V_{dc})^2$ dependence. The measurements indicate that the minimum detectable force for the present level of system noise is $\sim 10 \text{ nN}$. Note that the slopes of the curves for the two capacitors, which are proportional to $1/d^2$, are different implying that the sensor has a natural imbalance. The ratio of the slopes in Fig. 4 is 1.50 ± 0.05 , while the independently measured ratio d_1^2/d_2^2 is 1.40 ± 0.1 , in good agreement. These measurements also permit an experimental determination of the teeter-totter force constant yielding a value of $15 \pm 2 \text{ N/m}$ in excellent agreement with the 13 N/m value calculated earlier.

The ultimate test of the sensor is, of course, its ability to measure interfacial force profiles in the absence of the mechanical instability discussed earlier. The interfacial forces were measured with a W tip attached to a piezo drive which moves it in proximity to one end of the Be-Cu sensor. These tests were done in air so that both the tip and sensor are undoubtedly covered with oxide and water films. Scans were performed with and without feedback control.

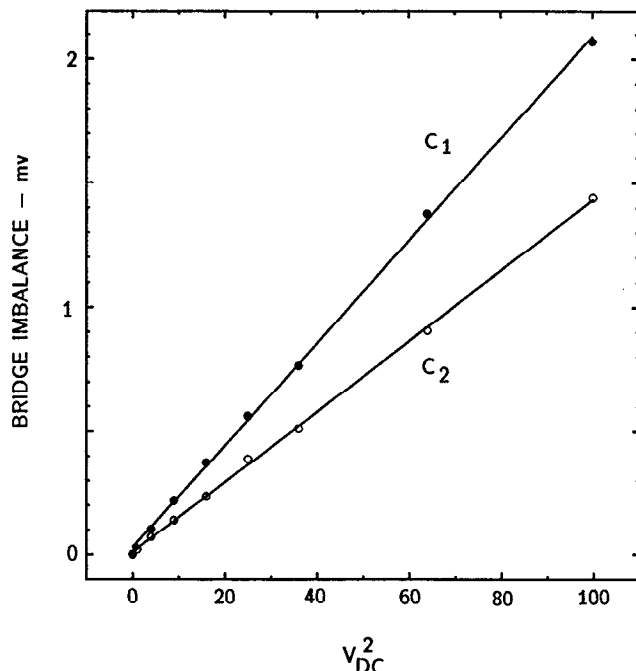


FIG. 4. The result of measurements of the bridge imbalance voltage caused by the application of a dc voltage to the individual capacitors. The linear curves show the expected quadratic dependence with applied dc voltage. The curves for the two capacitors have different slopes because of the natural imbalance of the sensor.

Shown in the top curve marked (a) in Fig. 5 are the force profiles as measured by the feedback output as the tip approaches and withdraws from the point of equilibrium force (the two curves are vertically displaced for clarity). The long-range nature of the forces indicates either a Van der Waal or capillary-type interaction.²³ There is no appreciable hysteresis between approach and withdrawal, indicating that only small, irreversible adhesion occurred; although hysteresis behavior is observed if one probes more deeply into the repulsive region. The bridge imbalance or sensor displacement during the scan is shown as the lower curve marked (a) in Fig. 5. As can be seen, the feedback maintains the sensor at its equilibrium position, within the noise level, throughout the entire scan.

The sensor displacement for the same system measured without feedback is shown as the lower curve marked (b) in Fig. 5. Upon approach, the teeter-totter deflects in response to the interfacial force. At a separation of $\sim 30 \text{ nm}$, the force gradient exceeds the force constant and the teeter-totter jumps into virtual contact with the tip. Further ramping simply results in a mechanical deflection of the sensor and a one-to-one relationship between piezo displacement and bridge imbalance. This contact is maintained up to the equilibrium force point where the motion is reversed. Subsequent withdrawal reveals significant hysteresis and a second jumping event at about 60 nm separation as shown by the x's in (b) of Fig. 5. This type of hysteresis has been observed and detailed by others.^{4,7,13} Again, it simply reflects the point at which $k = \partial F / \partial z$. For tip withdrawal, the instability occurs at a separation just

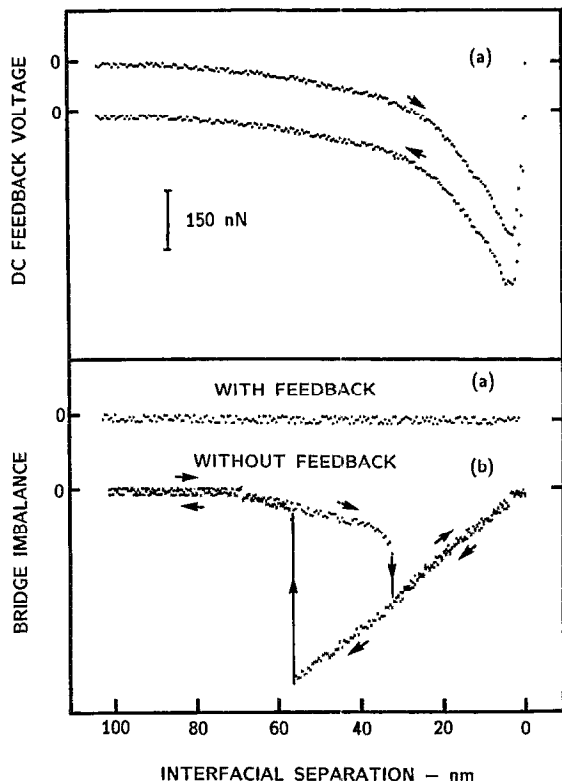


FIG. 5. The two plots indicated by (a) show the dc feedback voltage and bridge imbalance plotted as a function of the interfacial separation between a W tip and the BeCu sensor surface. The top curve illustrates the actual force profile for these two surfaces while the bottom (a) curve shows that the feedback keeps the bridge balanced, within the noise, over the entire excursion. The (b) curve indicates the bridge imbalance in the absence of feedback and illustrates the two instability points for the approach and withdrawal excursions.

beyond that corresponding to the maximum interfacial force. It is clear from Fig. 5 that without the force-feedback control a large percentage of the force profile is lost because of the mechanical instabilities of the displacement sensor.

V. DISCUSSION

We have described the conceptual design and prototype performance data for a new interfacial force microscope that employs an electrostatic force feedback sensor to circumvent the mechanical instability inherent in deflection-type force sensors. We have demonstrated the efficacy of the electrostatic feedback scheme utilizing a differential capacitor arrangement for the sensor itself. This sensor offers distinct advantages over other displacement detectors including: (1) electronic displacement detection and electrostatic feedback in the same compact unit, (2) the ability to impose both attractive and repulsive balancing forces, and (3) only second order sensitivities to both mechanical vibrations and electrical noise in the function generator driving the ac bridge circuit. While these are important advantages, they do not restrict the application of the electrostatic feedback technique to this sensor. For example, the placement of appropriate electrodes

around the cantilevers widely used in present-day AFM sensors could convert these units into active feedback force detectors. Furthermore, such an arrangement could be implemented with presently used displacement detection schemes; e.g., using field emission,¹ laser interferometer²⁶ or laser lever⁸ techniques as well as capacitance techniques.²⁰

The prototype unit discussed here was found to have force and displacement sensitivities of 10 nN and $\sim 5 \text{ \AA}$, respectively; values that are presently limited by system vibrations and extraneous electronic noise. Preliminary results demonstrate the force-feedback sensor's ability to measure interfacial-force profiles over their entire effective range, including interfacial contact. Although initial performance figures indicate that the prototype is adequate for studying interfacial bonding for a wide variety of interesting systems, significant improvement in performance can be achieved by careful attention to improving circuit noise and to enhancing teeter-totter stability in order to decrease the capacitor-plate spacing. In fact, it is reasonable to anticipate that sensors of this general type will eventually be among the most sensitive available for interfacial applications.²² Finally, we should point out that with the sample mounted on a three-axis piezo drive, the sensor readily lends itself to *x-y* scanning that will be able to form 3-D images for the full range of interfacial force—both attractive and repulsive.

ACKNOWLEDGMENTS

The authors wish to thank T. A. Michalske, T. Klitsner, and G. M. McClelland (IBM-Almaden) for many helpful discussions and B. J. Lammie and A. J. Ricco for the making of the thin film depositions.

- ¹G. Binnig, C. F. Quate, and C. Gerber, *Phys. Rev. Lett.* **12**, 930 (1986).
- ²U. Durig, J. K. Gimzewski and D. W. Pohl, *Phys. Rev. Lett.* **57**, 2403 (1986).
- ³C. M. Mate, G. M. McClelland, R. Erlandsson, and S. Chiang, *Phys. Rev. Lett.* **59**, 1942 (1987).
- ⁴Y. Martin, C. C. Williams, and H. K. Wickramasinghe, *J. Appl. Phys.* **61**, 4723 (1987).
- ⁵R. Erlandsson, G. Hadziioannou, C. M. Mate, G. M. McClelland, and S. Chiang, *J. Chem. Phys.* **89**, 5190 (1988).
- ⁶N. A. Burnham and R. J. Colton, *J. Vac. Sci. Technol. A* **7**, 2906 (1989).
- ⁷E. Meyer, H. Heinzelmann, P. Grutter, T. Jung, H. R. Hidber, H. Rudin and H. J. Guntherodt, *Thin Solid Films* **181**, 527 (1989).
- ⁸A. L. Weisenhorn, P. K. Hansma, T. R. Albrecht, and C. F. Quate, *Appl. Phys. Lett.* **54**, 2651 (1989).
- ⁹P. J. Bryant, H. S. Kim, R. H. Deeken, and Y. C. Cheng, *J. Vac. Sci. Technol. A* **8**, 3502 (1990).
- ¹⁰N. A. Burnham, D. D. Dominguez, R. L. Mowery, and R. J. Colton, *Phys. Rev. Lett.* **64**, 1931 (1990).
- ¹¹D. Tabor and R. H. S. Winterton, *Proc. R. Soc. London A* **312**, 435 (1969).
- ¹²J. N. Israelachvili, *Chemtracts* **1**, 1 (1989).
- ¹³K. B. Lodge, *Adv. Coll. Interface Sci.* **19**, 27 (1983).
- ¹⁴J. B. Pethica and A. P. Sutton, *J. Vac. Sci. Technol. A* **6**, 2490 (1988).
- ¹⁵U. Landman, W. D. Luedtke, and M. W. Ribarsky, *J. Vac. Sci. Technol. A* **7**, 2829 (1989).
- ¹⁶J. R. Smith, G. Bozzolo, A. Banerjee, and J. Ferrante, *Phys. Rev. Lett.* **63**, 1269 (1989).
- ¹⁷P. Taylor, J. Nelson, and B. Dodson (unpublished).
- ¹⁸B. V. Derjaguin, V. I. Rabinovich, and N. V. Churaev, *Nature* **272**, 313 (1978).

- ¹⁹H. K. P. Neubert, *Instrument Transducers, An Introduction to their Performance and Design* (Clarendon, Oxford, 1963).
- ²⁰G. Neubauer, S. R. Cohen, G. M. McClelland, D. Horne, and C. M. Mate, *Rev. Sci. Instrum.* **61**, 2296 (1990).
- ²¹T. Goddenhenrich, H. Lemke, U. Hartmann and C. Heiden, *J. Vac. Sci. Technol. A* **8**, 383 (1990).
- ²²V. B. Braginsky and A. B. Manukin, in *Measurement of Weak Forces in Physics Experiments*, edited by D. H. Douglass (University of Chicago, Chicago, 1977).
- ²³J. N. Israelachvili, *Intermolecular and Surface Forces* (Academic, London, 1985).
- ²⁴P. Horowitz and W. Hill, *The Art of Electronics* (Cambridge University Press, Cambridge, 1980), p. 120.
- ²⁵G. L. Miller, E. R. Wagner, and T. Sleater, *Rev. Sci. Instrum.* **61**, 1266 (1990).
- ²⁶D. Rugar, H. J. Mamin, and P. Guethner, *Appl. Phys. Lett.* **55**, 2588 (1989).